UNIVERSITY OF
FORWARD
THINKING
WESTMINSTER

WestminsterResearch
http://www.westminster.ac.uk/westminsterresearch

Reprogramming of hepatic fat accumulation and 'browning' of adipose tissue by the short-chain fatty acid acetate

Sahuri Arisoylu, M., Brody, L., Parkinson, J., Parkes, Harold G., Navaratnam, N., Miller, Andrew D., Thomas, E.L., Frost, G.S. and Bell, J.D.

This is an author's accepted manuscript of an article published in the *International Journal of Obesity* (12 February 2016) | doi:10.1038/ijo.2016.23. The final definitive version is available online at:https://dx.doi.org/10.1038/ijo.2016.23

The WestminsterResearch online digital archive at the University of Westminster aims to make the research output of the University available to a wider audience. Copyright and Moral Rights remain with the authors and/or copyright owners.

Whilst further distribution of specific materials from within this archive is forbidden, you may freely distribute the URL of WestminsterResearch: ((http://westminsterresearch.wmin.ac.uk/).

In case of abuse or copyright appearing without permission e-mail repository@westminster.ac.uk

Reprogramming of hepatic fat accumulation and “browning” of adipose tissue by the short chain fatty acid acetate

Acetate Re-engineers Fat Metabolism

Meliz Sahuri-Arisoylu[1,2,*], Leigh P. Brody[2,*], James R. Parkinson[1], Harry Parkes[3], Naveenan Navaratnam[4], Andrew D. Miller[5], E. Louise Thomas[1], Gary Frost[2], Jimmy D. Bell[1*]

1. Department of Life Sciences, Faculty of Science and Technology, University of Westminster, 115 New Cavendish Street, London, W1W 6UW, UK
2. Nutrition and Dietetic Research Group, Division of Diabetes, Endocrinology and Metabolism, Department of Investigative Medicine, Imperial College London, Hammersmith Hospital, London W12 0NN, UK
3. CR-UK Clinical MR Research Group, Institute of Cancer Research, Sutton, Surrey SM2 5NG, UK
4. Cellular Stress Group, MRC Clinical Sciences Centre, Imperial College London, Hammersmith Hospital, London W12 0NN, UK
5. Institute of Pharmaceutical Science, King's College London, Franklin-Wilkins Building, Waterloo Campus, 150 Stamford Street, London SE1 9NH, UK
6. These authors contributed equally to this work.

* Correspondence should be directed to J.D.B. (J.Bell@westminster.ac.uk)

ABSTRACT

BACKGROUND/OBJECTIVES: Short chain fatty acids (SCFA), produced by microbiome fermentation of carbohydrates, have been linked to a reduction in appetite, body weight and adiposity. However, determining the contribution of central and peripheral mechanisms to these effects has not been possible.

SUBJECTS/METHODS: C57BL6 mice fed with either normal or high fat diet (NFD and HFD, respectively) were treated with nanoparticle delivered acetate and the effects on metabolism were investigated.

RESULTS: In the liver, acetate decreased lipid accumulation and improved hepatic function, as well as increasing mitochondrial efficiency. In white adipose tissue, it inhibited lipolysis and induced “browning”, increasing thermogenic capacity which led to a reduction in body adiposity.

CONCLUSIONS: This study provides novel insights into the peripheral mechanism of action of acetate, independent of central action, including “browning” and enhancement of hepatic mitochondrial function.

INTRODUCTION

Obesity, arising from an imbalance between energy intake and energy expenditure, leads to a number of metabolic dysfunctions, including excess triglyceride synthesis and hepatic lipid accumulation (1). There is increasing evidence linking fermentable carbohydrates (FC) to the management of appetite regulation and negative energy balance in healthy and obese subjects (2-4). Several studies have shown that dietary supplementation of FC results in appetite suppression, reduced body adiposity, lower lipid accumulation in liver cells, as well as increased expression of anorexigenic gut hormones (3, 5-8). The consumption of FC results in the formation of SCFA mainly acetate, propionate and butyrate in the colon by microbiota. Butyrate is largely utilized as a substrate for colonocytes; propionate is taken up by the gut and mostly metabolized by the liver whereas acetate enters the peripheral

circulation (9). It has been suggested that increased production of SCFAs may play an important role in both satiety and adipose tissue (AT) remodeling (10).

Acetate is the main SCFA found in circulation and therefore the prime candidate to induce significant metabolic modulation in peripheral tissues. There is however conflicting evidence regarding the mechanism of action of acetate on lipid metabolism which may arise from its short half-life combined with the non-targeted nature of oral and peripheral administration. While some studies showed that administration of SCFAs acetate and propionate, inhibit lipolysis (11, 12), others have shown that acetate decreased fat accumulation through modification of either fatty acid oxidation (13) or fatty acid synthesis and AMP-activated protein kinase (AMPK) activity (14, 15) Recently, we have shown that acetate plays an important role in appetite suppression (16). Although we have found evidence to support a central mechanism for the mode of action of acetate, less is known regarding potential peripheral mechanisms.

In order to assess the peripheral action of acetate, herein we utilize a novel nanoparticle delivery method, whereby acetate is passively targeted to the periphery. Using this method we investigated the effects of acetate on liver lipid accumulation, inflammation and mitochondrial metabolism. Our findings suggest that the positive effects of acetate on liver lipid accumulation are as a result of mitochondrial modifications in both the liver and subcutaneous adipose tissue (SAT), leading to “browning” of SAT and an overall improvement in metabolism and body composition in the absence of changes in calorie intake or physical activity.

MATERIALS AND METHODS

Experimental Animals

All *in vivo* experiments were carried out in compliance with the Animals (Scientific Procedure) Act 1986. Mice were supplied by Harlan, UK and housed 4 per cage, in a temperature controlled room at approximately 21-23°C with alternating 12h periods of light

and dark (light: 7:00-19:00) in filter-topped cages with ad libitum access to water. NFD was the RM3 diet supplemented by Special Diet Services (Essex, UK). 60% of the caloric content of the HFD was fat (EF D12402; Special Diet Services).

Chronic Liposome encapsulated acetate (LITA) Nanoparticle Administration to C57BL/6 Mice Placed on a HFD or NFD

Male adult C57BL/6 mice were placed on either a HFD (n=48) or NFD (n=48) for 6 weeks. Within each dietary group mice received an intraperitoneal (i.p.) injection of either LITA nanoparticle (n=24) or control (HEPES) (n=24) three times per week. Whole body ^{1}H Magnetic resonance spectroscopy (MRS) and liver ^{1}H MRS were performed prior to dietary intervention and after 4 weeks of the start of the study to calculate whole body adiposity and intrahepatocellular lipid (IHCL) content, respectively. At the start of week 5, a fasted glucose tolerance test (GTT) was performed, (n=10-12) or animals went into Comprehensive Lab Animal Monitoring System (CLAMS, Columbus Instruments, USA) (n=8). After week 6 animals were euthanized; blood samples and organs, including the liver, epididymal, mesenteric and subcutaneous fat depots were collected and stored at -80°C for measurement of enzymes, markers and gene expression analysis. The details of all procedures are provided in the Supplementary Information.

Cell Culture

THLE-2 cells (ATCC® CRL-2706™) which are derived from normal human liver cells and transformed with SV40 large T antigen were purchased from ATCC and grown in BEBM medium supplemented with BEGM bullet kit (Lonza, Switzerland) at $37^{0}C$ with 5% CO_2 as per ATCC's instructions. A549 Parent (wild type) and rho0 (lacking mitochondrial DNA) lung cancer cells were grown in DMEM supplemented with uridine only for rho0 at $37^{0}C$ with 5% CO_2 as described in (17). Mitochondrial function of all cell types was assessed using a XF24 Analyzer (Seahorse Bioscience, USA). A detailed protocol is provided in the Supplementary Information.

Statistical Analysis

All statistical analyses were performed using GraphPad Prism (GraphPad Software, USA). Data are presented as means ± standard deviation (SD) except where stated as mean ± standard error of mean (SEM). Statistical significance was calculated with Student's t test or repeated measures ANOVA analysis where appropriate. Significance was accepted at the level of *=p<0.05, **=p< 0.01, ***=p<0.001.

RESULTS

Development of Nanoparticle Delivery System for Acetate

LITA (Supplementary Figure S1a) nanoparticles were prepared from lipids by thin film hydration method, then employed for the functional delivery of acetate to the main organs in the periphery following i.p. administration (16). To show that acetate is encapsulated in the liposomes we employed the affinity of albumin to bind ions and the fact that it is NMR "invisible". When acetate binds to albumin it becomes "invisible" to NMR (Supplementary Figure S1 b and c) but when acetate is encapsulated in the liposomes albumin cannot bind to it and the acetate peak is still visible (Supplementary Figure S1 d and e). The concentration of acetate was similar to physiological levels; in 200µl of LITA about 52.9µg (4.41mM) and the size of the liposomes were 102.3 ± 7.5nm and 95.9 ± 9.0nm for LITA and control liposomes respectively (p=0.6). 100nm is suggested as optimal size to create stable liposomes (18, 19).

Biodistribution to the liver, heart, muscle, spleen and lung was confirmed by histological analysis (making use of fluorescence tags, LITA-Rhd) at 2h post administration (Supplementary Figure S1f-j). Extended biodistribution at 24 and 48h post administration was assessed by magnetic resonance imaging (MRI), using a positive lipid-based contrast agents (LITA-Gd) (20). Increased uptake of LITA-Gd in liver was confirmed by the expected

reduction in T1 value (Supplementary Figure S1k). No change in brain T1 was observed (Supplementary Figure S1l). Overall these studies confirmed that only peripheral tissues were reached by the LITA nanoparticle. This is typical for nanoparticles of this type, confirming that LITA nanoparticles do not enter the brain. Therefore results obtained in this study would be independent of any potential appetite suppressing effect by acetate.

Acetate Reduces Whole Body and Ectopic Lipid Accumulation with No Reduction in Food Intake or Weight Gain

In order to assess the effects of acetate on overall metabolism, lean 8-week-old C57Bl/6 mice were put on NFD or HFD and were administered i.p. with Control or LITA nanoparticles 3 times per week for 6 weeks. Acetate administration in LITA nanoparticles reduced whole body adiposity significantly in HFD fed mice ($p<0.05$) with similar trend in NFD fed mice ($p<0.08$) (Figure 1a and 1b). No change was observed in the daily food intake of both groups, even so the NFD group showed an overall weight gain with LITA treatment (Supplementary Figure S2a-d). Furthermore, lean mass was significantly increased in the HFD fed group with LITA treatment ($p<0.05$) with a similar trend was observed in the NFD fed group ($p=0.07$, Figure 1c and 1d). Importantly, LITA treatment in both groups led to a reduced accumulation of IHCL in both groups ($p<0.05$, Figure 1e and 1f) compared with control nanoparticle treatment. Similar reductions were observed in whole body adiposity ($p<0.05$) and IHCL ($p<0.001$) with LITA treatment under a more robust model of obesity, where mice were fed with HFD for 5 weeks prior to treatment with LITA, (Supplementary Figure S2e and f) again these changes were independent of changes in food intake or weight gain (data not shown). Pancreatic triglyceride (TG) levels also exhibited a trend towards reduction in both groups (Supplementary Figure S2g)*.* No morphological abnormalities were observed in either group in the liver of LITA or control nanoparticle treated mice (Supplementary Figure S2h) nor were there significant changes observed in

weight of the liver or of pancreas (Supplementary Figure S2i and j), as well as the size or volume of adipocytes from SAT (Supplementary Figure S3a-e).

Acetate improves liver function

LITA treatment resulted in a reduction in aspartate aminotransferase (AST) and alkaline phosphatase (ALP) serum levels in the HFD group suggesting an improvement in liver function ($p<0.05$, Figure 2a). Similarly, there was a reduction in serum interleukin-6 (IL-6) and tumor necrosis factor-α (TNF-α) concentrations in HFD fed mice treated with LITA, though this did not reach significance ($p<0.07$, Figure 2b). This was associated with a reduction in *TNF-α* expression in both the liver ($p<0.01$) and SAT ($p<0.001$) (Figure 2c). No change was observed in liver function enzymes of NFD mice treated with LITA but a significantly lower serum concentration of TNF-α ($p<0.01$) and reduced expression of TNF-α in the liver ($p<0.05$) was observed (Figure 2d and 2e). These changes are significant since pro-inflammatory cytokines such as TNF-α and IL-6 are believed to trigger inflammation in the liver following lipid accumulation, leading to liver fibrosis (21). No changes were observed in monocyte chemoattractant protein-1 (MCP-1) or resistin in both cohorts (Figure 2f and 2g)

Glucose metabolism is altered by acetate

No change was observed in the recovery of blood glucose to baseline level after GTT in NFD (Figure 3a and 3b) or HFD (Figure 3c and 3d). In NFD cohort, homeostatic model assessment of insulin resistance (HOMA-IR) was significantly reduced with acetate treatment (Figure 3e and 3g). In HFD cohort, the fasted level of glucose dropped less, with no change in fasted insulin and fed insulin levels were lower ($p<0.05$) with no change in fed glucose (Figure 3f and 3g). The gene expression of glucose transporter 2 (GLUT2) in HFD cohort, was significantly reduced with LITA treatment ($p<0.01$, Fig. 3h). Serum glucagon levels showed a significant increase with LITA administration compared to control in HFD fed mice ($p<0.05$, Figure 2g), possibly due to reduced insulin levels.

Acetate reduces AT lipolysis, circulating free fatty acid (FFA) levels and de-novo lipogenesis in liver

In HFD fed mice, the gene expression of adipose tissue triglyceride lipase (*ATGL*), which breaks down TG into diacylglycerols and FFAs (22) was reduced with LITA (Figure 4a), correlating with reduced circulating levels of serum FFAs ($p<0.05$, Figure 4b). Similarly, mRNA expression of genes in liver involved in de-novo lipogenesis, namely sterol regulatory element-binding protein 1 (*SREBP1*), Fatty acid synthase (*FASN*) and Acetyl-CoA carboxylase (*ACC*), were significantly reduced following LITA treatment ($p<0.01$, Figure 4c). These reductions in circulating serum FFAs, due to reduced SAT-based lipolysis, together with reductions in de-novo lipogenesis could certainly offer explanation for the observed reduction in IHCL with LITA treatment. These effects appear to be balanced by LITA treatment induced reductions in fatty acid oxidation and VLDL export compared to control, as reflected by downregulation in expression of fatty acid oxidation genes carnitine palmitoyltransferase I (*CPT1*, $p<0.01$) and acyl-CoA oxidase 1 (*ACOX*, $p<0.05$) and VLDL synthesis ($p<0.001$). These latter data are in line with reduced FFAs reaching the liver.

Acetate improves liver mitochondrial function and increases ATP production

Impaired mitochondrial metabolism is an underlining cause for a number of diseases including fatty liver (23). Initially, liver mitochondria were assessed using transmission electron microscopy (TEM). No change was observed in the number of mitochondria (Figure 5a and 5b) while genes involved in the mitochondrial biogenesis remained unaffected (Figure 5e). However, a trend towards increasing numbers of cristae per mitochondria was observed ($p<0.07$, Figure 5c and 5d). As cristae are the sites for electron transport chain (ETC), protein expression of these complexes was investigated. Significant increases in the expression of complexes III, IV and V were detected ($p<0.05$, $p<0.01$ and $p<0.001$, respectively, Figure 5f and 5h). Moreover there was a significant reduction in expression levels of uncoupling protein 2 (*UCP2*, $p<0.05$, Figure 5E)**,** suggesting a less “leaky” mitochondrial membrane, providing more electrons for the ETC and increased ATP

production. In order to further assess the potential effect of acetate on ATP production, immortal non-cancerous hepatocytes (THLE-2, an in vitro model for normal liver cells) were treated with acetate and oxygen consumption rate (OCR) was monitored using a XF-analyzer. Basal respiration and ATP production were significantly increased by acetate. (Figure 5g).

Acetate increases thermogenic capacity through “browning” of white adipose tissue (WAT)

HFD and NFD fed mice treated with LITA or its control counterpart underwent physiological analysis by CLAMS. Acetate administration by LITA nanoparticle increased heat production in both HFD ($p<0.01$, Figure 6a and 6b) and NFD ($p<0.05$, Figure 6c and 6d) fed mice. Recently it has been shown that WAT depots can be “browned” by activators such as cold (24-27). ‘Beige’ or ‘brite’ adipocytes have more abundant mitochondria compared to white adipocytes, thus increasing thermogenic potential (28). Since we observed increased thermogenic output in the LITA treated animals, gene expression of UCP1 in SAT was investigated. In the HFD cohort, *UCP1* expression was significantly increased ($p<0.001$, Figure 6e). We then went on to assess peroxisome proliferator activated receptor gamma coactivator 1 alpha (*PGC1α*) and PR domain containing 16 (*PRDM16*) to confirm the possibility of “browning” of WAT as both are involved in the differentiation of brown-like adipocytes (25, 29). *PRDM16* was significantly increased ($p<0.001$), while *PGC1α* showed a similar trend (Figure 6E). In the NFD cohort a significant increase in PRDM16 ($p<0.001$) expression was also observed, while *UCP1* and *PGC1α* expressions remained unchanged (Figure 6f). These changes occurred independent of changes in size or *UCP1* expression of brown adipose tissue (BAT, the AT depot behind the neck of mice), the main site for heat production (Figure 6g and 6h). In both cohorts VO_2 and VCO_2 trended to be higher but did not reach significance and physical activity was unaffected by LITA treatment (Supplementary Figure S4 and S5, NFD and HFD respectively).

Positive effects of acetate are lost in the presence of dysfunctional mitochondria

Rho0 cells, derived from A549 lung cancer cells, lack mitochondrial DNA (17), and are deficient in proteins of respiratory complexes I, III, IV and V (30) (Supplementary Figure S6a). Rho0 cells and wild type A549 cells (parent) were treated with 1mM acetate leading to increased ATP-linked respiration in 'parent' cells ($p=0.06$) whereas this effect was absent in Rho0 cells ($p<0.4$, Supplementary Figure S6b and c). In order to confirm *in vivo* that the beneficial effects of acetate on adiposity and inflammation was mediated by mitochondria, a group of mice were put on methionine choline deficient diet (MCD) and treated with LITA versus control nanoparticles. Mice on MCD have been previously shown to have impaired mitochondrial function and increased liver inflammation (31). No reversal in liver fat accumulation or body adiposity was observed following LITA treatment (Supplementary Figure S6d). In addition serum inflammatory markers remained unchanged by LITA treatment (Supplementary Figure S6e) confirming that acetate requires functional mitochondria to exert its beneficial effects.

DISCUSSION

In this study we make novel mechanistic insights into the peripheral effects of the SCFA acetate, following its delivery by a nanoparticle mediated system. The beneficial peripheral phenotypic effects of acetate are clearly independent of its effect on brain, where it is also known to be active (16). Our results reveal for the first time that acetate stimulates a number of autonomous mechanisms in different peripheral tissues. In the liver it reduces fat deposition through a reduction in circulating FFAs and de-novo lipogenesis and an increase in mitochondrial efficiency, while in adipose tissue it induces "browning", leading to a contraction in body adiposity.

Peripheral administration (oral/i.p.) of acetate has been previously shown to result in non-targeted uptake, rapid clearance from the circulation and reduced pH (32). Lipid based

nanoparticles (LNP) such as LITA can be used to target drugs to tissues (33) and have been employed in our lab to mediate functional siRNA delivery (34), as well as MRI contrast-agents, to tumors (18, 20). By adopting this methodology we passively target the liposomes to peripheral tissues and increase the bioavailability of acetate. This enables *in vivo* studies of the mechanism underlying the action of individual SCFA (separately or in combination) to be undertaken in a more controlled manner. This is important as recent work suggest that propionate and butyrate have very distinctive metabolic effects (35). Furthermore, our methodology allows for a separation of peripheral and central effects of acetate.

Our data herein shows that acetate reduces whole body fat without a decrease in caloric intake or weight gain. Previously, Yamashita et al have reported reduced food intake and weight in mice that received acetate orally (14) however, like others, their experimental design made it impossible to disassociate central from peripheral effects. Indeed, we recently demonstrated the central mechanism underpinning the appetite suppressing effect of acetate, and how this effect is lost when acetate is encapsulated in liposomes (16). Thus, the use of a LNP delivery system in our study enabled us to investigate the effect of acetate independent of its appetite suppressing action, which partly explain the lack of weight change reported by others (13, 14). Furthermore, the decrease in adiposity observed in our study was accompanied by an increase in lean mass, which would in turn balance changes in overall weight.

We have also observed that acetate treatment reduces ectopic fat accumulation firstly by reducing lipolysis (11) through a reduction in expression of ATGL in SAT *(22)*, which correlates with the observed reduction in serum FFA concentration. Reduced circulating FFAs then ameliorate hepatic exposure resulting in reduced TG synthesis and deposition in liver. This finding is supported by a recent report that FFA is the main mechanism responsible for TG synthesis in the liver (36). Furthermore, we also see a reduction in insulin which is known to regulate de-novo lipogenesis in the liver through its action on SREBP1 (37). Suppression of *SREBP1* expression and lowering glucose uptake by the liver, shown by reduced *GLUT2* expression, is known to reduce de-novo lipogenesis (38).

Together with *SREBP1*, the expression of downstream genes *FASN* and *ACC* was concomitantly reduced. Recent studies have suggested that acetate in the liver is converted into acetyl-coA in the cytoplasm through *ACSS2* and synthesized to long chain fatty acids (39). However, in our study we show that chronic treatment with acetate suppresses the expression of *ACSS2*, together with lipid synthesis and it increases the expression of oxidative phosphorylation (OXPHOS) proteins suggesting improved mitochondrial metabolism.

Glucose metabolism was also affected by acetate treatment. Reduced insulin and maintained glucose concentrations in fed state suggest acetate improves insulin sensitivity. In the fasted state, the drop in blood glucose levels in mice treated with LITA nanoparticles was not as pronounced as in mice treated with control nanoparticles. This is contrary to findings of Yamashita et al who reported a reduction in fasting glucose with acetate treatment, although their use of a diabetic rat model may account for these differences (14). In addition, the observed reduction in expression of *GLUT2* following LITA treatment, together with reduced serum insulin and a less enhanced drop in blood glucose in the fasted state, are consistent with changes in the liver fuel source away from glucose. This is in agreement with the Randle hypothesis (40) that links fatty acids to inhibition of glucose oxidation.

Mitochondria, which are at the center of fatty acid metabolism and oxidative phosphorylation, play a key role in hepatocyte function (23). Mitochondrial dysfunction is also closely linked to the pathogenesis of non-alcoholic fatty liver disease (NAFLD) (41). Furthermore, increased *UCP2* expression has been associated with non-alcoholic steatohepatitis (NASH) development (42) and lipid accumulation reduces the efficiency of OXPHOS in liver (43). In our study we have observed reduced *UCP2* expression in LITA treated mice together with increased protein expression of OXPHOS complexes. In immortal THLE-2 cells ATP-linked respiration is increased with acetate treatment. Furthermore, when mitochondrial function is impaired (in Rho0 cells, by deletion of mitochondrial DNA and *in vivo,* by feeding a MCD) ATP production and liver fat accumulation remain unaffected by LITA treatment. This strong

evidence that enhancement in mitochondrial function is pivotal to the prevention of NAFLD by acetate. Although *in vitro*, lung cancer cells were used instead of liver cells, A549 cells still carry out beta-oxidation (44) which makes them a good model for investigating the effect of acetate on mitochondria function.

Mitochondrial modulations in adipose tissue may also explain how acetate reduces whole body adiposity without appetite suppression. Acetate treatment causes increased thermogenic capacity in mice, independent of BAT, through the process of “browning” of WAT. It has been recently shown that heat dissipation by browning of WAT plays a greater role in the management of obesity than the BAT itself (45, 46). This is in line with reports that mice lacking the mitochondrial acetyl-CoA synthatase 1 (*ACSS1*) are hypothermic when fasted (47). However, it is not clear whether the “browning process” in this study is a direct effect of acetate or due to the effects of reduced overall adiposity, which may in turn lead to “browning” of WAT (48). Similarly, the observed increase in lean mass may contribute to overall energy expenditure and reduce AT content (49). Moreover, inhibition of gluconeogenesis has been recently linked with increased energy expenditure (50). Since acetate appears to reduce liver glucose production, this should also be investigated as a potential route of action.

The overall benefits of acetate on the liver are strongly supported by reduced expression of *TNF-α* and lower serum TNF-α and IL6, suggesting less basal inflammation (51, 52). In addition, the reduction in serum AST and ALP levels, which are normally associated with NAFLD (53), are a strong indicator of hepatocellular damage. Although these changes were observed at an early stage of high fat feeding, they do suggest that LITA treatment may help to prevent the onset of NAFLD. In fact, when mice were fed with HFD for 5 weeks prior to treatment with LITA, significant reduction in IHCL level was observed. Furthermore, reduced levels of inflammation, serum insulin, serum FFAs and liver fat are all implicated in minimizing progression towards tumorigenesis (54, 55). The effect of acetate on tumorigenesis should also be investigated.

In conclusion, our study demonstrates significant peripheral effects of acetate on lipid metabolism, independent of its central action. Acetate administration via LNP reduces ectopic lipid accumulation through suppression of lipolysis in adipose tissue and by reducing de-novo lipogenesis in liver. We have demonstrated for the first time that acetate modulates mitochondrial function in liver, increasing OXPHOS and ATP production, and in the SAT increasing thermogenic activity. Our findings show that acetate has the potential to be a novel and effective treatment for obesity and fatty liver disease.

CONFLICT OF INTEREST

The authors declare no conflict of interest.

ACKNOWLEDGEMENTS

We thank Prof Alice Warley and Dr Gema Vizcay-Barrena from Centre for Ultrastructural Imaging where TEM was carried out. A549 lung cancer cell lines (Parent and Rho0) were a kind gift from Dr. Zhi Yao and Dr Gyorgy Szabadkai. This research was funded by Medical Research Council, UK.

AUTHOUR CONTRIBUTIONS

JDB, GF, ELT and MSA designed the experiments and wrote the manuscript. MSA performed and analyzed most of the experiments. MSA, LB ADM performed liposome formulation and delivery experiments. HP carried out NMR scans. NN conducted protein expression of A549 cells. All the authors (MSA, LPB, JRP, HP, NN, ADM, ELT GF, JDB) provided critical feedback in preparation and writing the manuscript.

Supplementary Information accompanies this paper on International Journal of Obesity website (http://www.nature.com/ijo)

REFERENCES

1. Eriksson S, Eriksson KF, Bondesson L. Nonalcoholic steatohepatitis in obesity: a reversible condition. Acta medica Scandinavica. 1986;220(1):83-8. Epub 1986/01/01.
2. Parnell JA, Reimer RA. Weight loss during oligofructose supplementation is associated with decreased ghrelin and increased peptide YY in overweight and obese adults. Am J Clin Nutr. 2009;89(6):1751-9.
3. Cani PD, Joly E, Horsmans Y, Delzenne NM. Oligofructose promotes satiety in healthy human: a pilot study. European Journal of Clinical Nutrition. 2006;60(5):567-72.
4. Pasman WJ, Saris WH, Wauters MA, Westerterp-Plantenga MS. Effect of one week of fibre supplementation on hunger and satiety ratings and energy intake. Appetite. 1997;29(1):77-87. Epub 1997/08/01.
5. So PW, Yu WS, Kuo YT, Wasserfall C, Goldstone AP, Bell JD, et al. Impact of resistant starch on body fat patterning and central appetite regulation. PLoS One. 2007;2(12):e1309. Epub 2007/12/13.
6. Keenan MJ, Zhou J, McCutcheon KL, Raggio AM, Bateman HG, Todd E, et al. Effects of resistant starch, a non-digestible fermentable fiber, on reducing body fat. Obesity (Silver Spring). 2006;14(9):1523-34. Epub 2006/10/13.
7. Cani P, Neyrinck A, Maton N, Delzenne N. Oligofructose promotes satiety in rats fed a high-fat diet: involvement of glucagon-like Peptide-1. Obesity research. 2005;13(6):1000-7.
8. Anastasovska J, Arora T, Sanchez Canon GJ, Parkinson JR, Touhy K, Gibson GR, et al. Fermentable carbohydrate alters hypothalamic neuronal activity and protects against the obesogenic environment. Obesity (Silver Spring). 2012;20(5):1016-23. Epub 2012/02/11.
9. Cummings JH, Pomare EW, Branch WJ, Naylor CP, Macfarlane GT. Short chain fatty acids in human large intestine, portal, hepatic and venous blood. Gut. 1987;28(10):1221-7. Epub 1987/10/01.
10. Robertson MD. Metabolic cross talk between the colon and the periphery: implications for insulin sensitivity. The Proceedings of the Nutrition Society. 2007;66(3):351-61.
11. Ge H, Li X, Weiszmann J, Wang P, Baribault H, Chen JL, et al. Activation of G protein-coupled receptor 43 in adipocytes leads to inhibition of lipolysis and suppression of plasma free fatty acids. Endocrinology. 2008;149(9):4519-26. Epub 2008/05/24.
12. Hong YH, Nishimura Y, Hishikawa D, Tsuzuki H, Miyahara H, Gotoh C, et al. Acetate and propionate short chain fatty acids stimulate adipogenesis via GPCR43. Endocrinology. 2005;146(12):5092-9. Epub 2005/08/27.
13. Kondo T, Kishi M, Fushimi T, Kaga T. Acetic Acid Upregulates the Expression of Genes for Fatty Acid Oxidation Enzymes in Liver To Suppress Body Fat Accumulation. Journal of Agricultural and Food Chemistry. 2009;57(13):5982-6.
14. Yamashita H, Fujisawa K, Ito E, Idei S, Kawaguchi N, Kimoto M, et al. Improvement of Obesity and Glucose Tolerance by Acetate in Type 2 Diabetic Otsuka Long-Evans Tokushima Fatty (OLETF) Rats. Bioscience, Biotechnology, and Biochemistry. 2007;71(5):1236-43.
15. Yamashita H, Maruta H, Jozuka M, Kimura R, Iwabuchi H, Yamato M, et al. Effects of Acetate on Lipid Metabolism in Muscles and Adipose Tissues of Type 2 Diabetic Otsuka Long-Evans Tokushima Fatty (OLETF) Rats. Bioscience, Biotechnology, and Biochemistry. 2009;73(3):570-6.
16. Frost G, Sleeth ML, Sahuri-Arisoylu M, Lizarbe B, Cerdan S, Brody L, et al. The short-chain fatty acid acetate reduces appetite via a central homeostatic mechanism. Nat Commun. 2014;5:3611. Epub 2014/05/02.

17. Lo S, Tolner B, Taanman JW, Cooper JM, Gu M, Hartley JA, et al. Assessment of the significance of mitochondrial DNA damage by chemotherapeutic agents. International journal of oncology. 2005;27(2):337-44. Epub 2005/07/13.
18. Kamaly N, Kalber T, Thanou M, Bell JD, Miller AD. Folate receptor targeted bimodal liposomes for tumor magnetic resonance imaging. Bioconjugate chemistry. 2009;20(4):648-55. Epub 2009/04/17.
19. Kostarelos K, Miller AD. Synthetic, self-assembly ABCD nanoparticles; a structural paradigm for viable synthetic non-viral vectors. Chemical Society reviews. 2005;34(11):970-94. Epub 2005/10/22.
20. Kalber TL, Kamaly N, So PW, Pugh JA, Bunch J, McLeod CW, et al. A low molecular weight folate receptor targeted contrast agent for magnetic resonance tumor imaging. Mol Imaging Biol. 2011;13(4):653-62. Epub 2010/09/03.
21. Tilg H, Moschen AR. Insulin resistance, inflammation, and non-alcoholic fatty liver disease. Trends Endocrinol Metab. 2008;19(10):371-9.
22. Zechner R, Zimmermann R, Eichmann TO, Kohlwein SD, Haemmerle G, Lass A, et al. FAT SIGNALS--lipases and lipolysis in lipid metabolism and signaling. Cell Metab. 2012;15(3):279-91. Epub 2012/03/13.
23. Wei YZ, Rector RS, Thyfault JP, Ibdah JA. Nonalcoholic fatty liver disease and mitochondrial dysfunction. World J Gastroentero. 2008;14(2):193-9.
24. Lee P, Linderman JD, Smith S, Brychta RJ, Wang J, Idelson C, et al. Irisin and FGF21 are cold-induced endocrine activators of brown fat function in humans. Cell Metab. 2014;19(2):302-9.
25. Boström P, Wu J, Jedrychowski MP, Korde A, Ye L, Lo JC, et al. A PGC1-α-dependent myokine that drives brown-fat-like development of white fat and thermogenesis. Nature. 2012;481(7382):463-8.
26. Fisher FM, Estall JL, Adams AC, Antonellis PJ, Bina HA, Flier JS, et al. Integrated regulation of hepatic metabolism by fibroblast growth factor 21 (FGF21) in vivo. Endocrinology. 2011;152(8):2996-3004. Epub 2011/06/30.
27. Emanuelli B, Vienberg SG, Smyth G, Cheng C, Stanford KI, Arumugam M, et al. Interplay between FGF21 and insulin action in the liver regulates metabolism. J Clin Invest. 2014;124(2):515-27. Epub 2014/01/10.
28. Harms M, Seale P. Brown and beige fat: development, function and therapeutic potential. Nature medicine. 2013;19(10):1252-63. Epub 2013/10/09.
29. Seale P, Conroe HM, Estall J, Kajimura S, Frontini A, Ishibashi J, et al. Prdm16 determines the thermogenic program of subcutaneous white adipose tissue in mice. J Clin Invest. 2011;121(1):96-105.
30. Schon EA, DiMauro S, Hirano M. Human mitochondrial DNA: roles of inherited and somatic mutations. Nature reviews Genetics. 2012;13(12):878-90. Epub 2012/11/17.
31. Varela-Rey M, Embade N, Ariz U, Lu SC, Mato JM, Martinez-Chantar ML. Non-alcoholic steatohepatitis and animal models: understanding the human disease. Int J Biochem Cell Biol. 2009;41(5):969-76. Epub 2008/11/26.
32. Cummings JH. Short chain fatty acids in the human colon. Gut. 1981;22(9):763-79. Epub 1981/09/01.
33. Miller AD. Delivery of RNAi therapeutics: work in progress. Expert review of medical devices. 2013;10(6):781-811. Epub 2013/11/08.
34. Kenny GD, Kamaly N, Kalber TL, Brody LP, Sahuri M, Shamsaei E, et al. Novel multifunctional nanoparticle mediates siRNA tumour delivery, visualisation and therapeutic tumour reduction in vivo. J Control Release. 2011;149(2):111-6. Epub 2010/10/05.
35. Canfora EE, Jocken JW, Blaak EE. Short-chain fatty acids in control of body weight and insulin sensitivity. Nature reviews Endocrinology. 2015;11(10):577-91. Epub 2015/08/12.
36. Vatner DF, Majumdar SK, Kumashiro N, Petersen MC, Rahimi Y, Gattu AK, et al. Insulin-independent regulation of hepatic triglyceride synthesis by fatty acids. Proceedings of the National Academy of Sciences of the United States of America. 2015;112(4):1143-8. Epub 2015/01/08.

37. Raghow R, Yellaturu C, Deng X, Park EA, Elam MB. SREBPs: the crossroads of physiological and pathological lipid homeostasis. Trends in endocrinology and metabolism: TEM. 2008;19(2):65-73. Epub 2008/02/23.
38. Prip-Buus C, Perdereau D, Foufelle F, Maury J, Ferre P, Girard J. Induction of fatty-acid-synthase gene expression by glucose in primary culture of rat hepatocytes. Dependency upon glucokinase activity. European journal of biochemistry / FEBS. 1995;230(1):309-15. Epub 1995/05/15.
39. Comerford SA, Huang Z, Du X, Wang Y, Cai L, Witkiewicz AK, et al. Acetate dependence of tumors. Cell. 2014;159(7):1591-602. Epub 2014/12/20.
40. Hue L, Taegtmeyer H. The Randle cycle revisited: a new head for an old hat. Am J Physiol Endocrinol Metab. 2009;297(3):E578-91. Epub 2009/06/18.
41. Pessayre D, Fromenty B. NASH: a mitochondrial disease. J Hepatol. 2005;42(6):928-40.
42. Serviddio G, Bellanti F, Tamborra R, Rollo T, Capitanio N, Romano AD, et al. Uncoupling protein-2 (UCP2) induces mitochondrial proton leak and increases susceptibility of non-alcoholic steatohepatitis (NASH) liver to ischaemia-reperfusion injury. Gut. 2008;57(7):957-65. Epub 2008/03/01.
43. Teodoro J, Rolo AP, Oliveira PJ, Palmeira CM. Decreased ANT content in Zucker fatty rats: relevance for altered hepatic mitochondrial bioenergetics in steatosis. FEBS Lett. 2006;580(8):2153-7. Epub 2006/03/24.
44. Harris FT, Rahman SM, Hassanein M, Qian J, Hoeksema MD, Chen H, et al. Acyl-coenzyme A-binding protein regulates Beta-oxidation required for growth and survival of non-small cell lung cancer. Cancer prevention research. 2014;7(7):748-57. Epub 2014/05/14.
45. Cohen P, Levy JD, Zhang Y, Frontini A, Kolodin DP, Svensson KJ, et al. Ablation of PRDM16 and beige adipose causes metabolic dysfunction and a subcutaneous to visceral fat switch. Cell. 2014;156(1-2):304-16. Epub 2014/01/21.
46. Harms MJ, Ishibashi J, Wang W, Lim HW, Goyama S, Sato T, et al. Prdm16 is required for the maintenance of brown adipocyte identity and function in adult mice. Cell Metab. 2014;19(4):593-604. Epub 2014/04/08.
47. Sakakibara I, Fujino T, Ishii M, Tanaka T, Shimosawa T, Miura S, et al. Fasting-induced hypothermia and reduced energy production in mice lacking acetyl-CoA synthetase 2. Cell Metab. 2009;9(2):191-202. Epub 2009/02/04.
48. Nedergaard J, Cannon B. The Browning of White Adipose Tissue: Some Burning Issues. Cell Metab.20(3):396-407.
49. Dolezal BA, Potteiger JA. Concurrent resistance and endurance training influence basal metabolic rate in nondieting individuals. Journal of applied physiology. 1998;85(2):695-700. Epub 1998/08/04.
50. Abdul-Wahed A, Gautier-Stein A, Casteras S, Soty M, Roussel D, Romestaing C, et al. A link between hepatic glucose production and peripheral energy metabolism via hepatokines. Molecular Metabolism. 2014;3(5):531-43.
51. Cox MA, Jackson J, Stanton M, Rojas-Triana A, Bober L, Laverty M, et al. Short-chain fatty acids act as antiinflammatory mediators by regulating prostaglandin E(2) and cytokines. World J Gastroenterol. 2009;15(44):5549-57. Epub 2009/11/26.
52. Reisenauer CJ, Bhatt DP, Mitteness DJ, Slanczka ER, Gienger HM, Watt JA, et al. Acetate supplementation attenuates lipopolysaccharide-induced neuroinflammation. J Neurochem. 2011;117(2):264-74. Epub 2011/01/29.
53. Wu TC, Chen LK, Tsai SH, Liaw YH, Hwang B. Hepatic steatosis: an experimental model for quantification. Arch Gerontol Geriatr. 2011;52(2):164-6. Epub 2010/04/20.
54. Sun B, Karin M. Obesity, inflammation, and liver cancer. J Hepatol. 2012;56(3):704-13. Epub 2011/11/29.
55. Khandekar MJ, Cohen P, Spiegelman BM. Molecular mechanisms of cancer development in obesity. Nat Rev Cancer. 2011;11(12):886-95. Epub 2011/11/25.

Figure Legends

Figure 1. Acetate Reduces Whole Body and Liver Lipid Accumulation

Change in whole body lipid content in HFD (**a**) and NFD (**b**) fed mice treated with and without LITA (n=24). Lean mass of control and LITA treated mice fed with HFD (**c**) and NFD (**d**) (n=8). Change in liver lipid content in HFD (**e**) and NFD (**f**) fed mice treated with and without LITA (n=24). All data are shown as mean ± SD, *p<0.05.

Figure 2. Acetate Improves Liver Function and Inflammation

(**a**) Serum concentration of ALT, AST and ALP of control and LITA treated mice under HFD feeding (n=12). (**b**) Inflammatory markers TNF-α and IL-6 of control and LITA treated mice under HFD feeding (n=18). (**c**) Fold change in LITA TNF-α expression compared to control in liver and SAT of mice fed with HFD. Dotted line represents control (n=6). (**d**) Serum concentration of ALT, AST and ALP of control and LITA treated mice under NFD feeding (n=6). (**e**) Fold change in LITA TNF-α expression from control (represented by dotted line) in liver of mice fed with NFD (n=6). (**f**) Serum concentration of peptides of control and LITA administered mice on NFD diet (n=18). (**g**) Concentration of other serum peptides of mice fed with HFD (n=18). All data are shown as mean ± SD, #p<0.1, *p<0.05, **p<0.01 and ***p<0.001.

Figure 3. Glucose Metabolism is Altered by Acetate

(**a**) Blood glucose concentration of control and LITA administered mice fed with NFD after i.p. glucose administration. (**b**) Area under the curve of blood glucose concentrations (n=10).

(**c**) Blood glucose concentration of control and LITA administered mice fed with HFD after i.p. glucose administration. (**d**) Area under the curve of blood glucose concentrations (n=10). (**e**) Fed and fasted blood glucose (n=24 and 18, respectively) and serum insulin concentrations (n=6 and 8, respectively) for control and LITA administered mice fed with NFD. (**f**) Fed and fasted blood glucose (n=36 and 22, respectively) and serum insulin concentrations (n=18 and 12, respectively) for control and LITA administered mice fed with HFD. (**g**) HOMA-IR for control and LITA administered mice fed with NFD (n=6) and HFD (n=12). (**h**) Fold change in LITA gene expression compared to control (represented by dotted line) in liver of mice fed with HFD (n=6). All data are shown as mean ± SD, *p<0.05 and **p<0.01.

Figure 4. Acetate Suppresses SAT Lipolysis and Liver de-novo Lipogenesis

(**a**) Fold change in LITA mRNA expression of genes involved in lipolysis compared to control (represented by dotted line) in SAT of mice fed with HFD (n=6). (**b**) Serum lipid concentrations of control and LITA administered mice fed with HFD (n=11). (**c**) Fold change in LITA mRNA expression of genes involved in fatty acid synthesis, β-oxidation and VLDL metabolism compared to control (represented by dotted line) in liver of mice fed with HFD (n=6). All data are shown as mean ± SD, *p<0.05, **p<0.01 and ***p<0.001.

Figure 5. Acetate Improves Liver Mitochondrial Function

(**a**) Representative TEM image of liver at 1200x magnification used to count the number of mitochondria. (**b**) Number of mitochondria per image of control and LITA administered mice fed on HFD (n=4). (**c**) A representative TEM image at 4800x magnification used to calculate the number cristae per mitochondrion. (**d**) Number of cristae per mitochondrion of control and LITA administered mice fed on HFD (n=3). (**e**) Fold change in LITA mRNA expression of genes involved in mitochondrial function compared to control (represented by dotted line) in liver of mice fed with HFD (n=6). (**f**) Change in protein expression of OXPHOS complexes of

mitochondria isolated from the liver of control and LITA administered mice (n=5). (**g**) Mitochondrial function, assessed by OCR, of THLE-2 cells treated with acetate 6 times, normalized to untreated cells (represented by dotted line, n=4). (**h**) Representative WB image showing complexes I-V. All data are shown as mean ± SD, #p<0.1, *p<0.05, **p<0.01 and ***p<0.001.

Figure 6. Acetate Increases Heat Dissipation through Browning of SAT

Heat produced measured by CLAMS of control and LITA administered mice fed with HFD shown as time course (**a**) and sum of light and dark phases (**b**) (n=8). Heat produced measured by CLAMS of control and LITA administered mice fed with NFD shown as time course (**c**) and sum of light and dark phases (**d**) (n=8). Fold change in LITA mRNA expression of BAT signature genes compared to control (represented by dotted line) in SAT of mice fed with HFD (n=6) (**e**) of mice fed with NFD (n=6) (**f**) and in BAT of mice fed with HFD (**g**). (**h**) Weight of BAT tissue dissected from the NFD and HFD fed mice (n=12). All data are shown as mean ± SD except from (a) and (c) which are shown as mean ± SEM, *p<0.05, **p<0.01 and ***p<0.001.

Figure 1

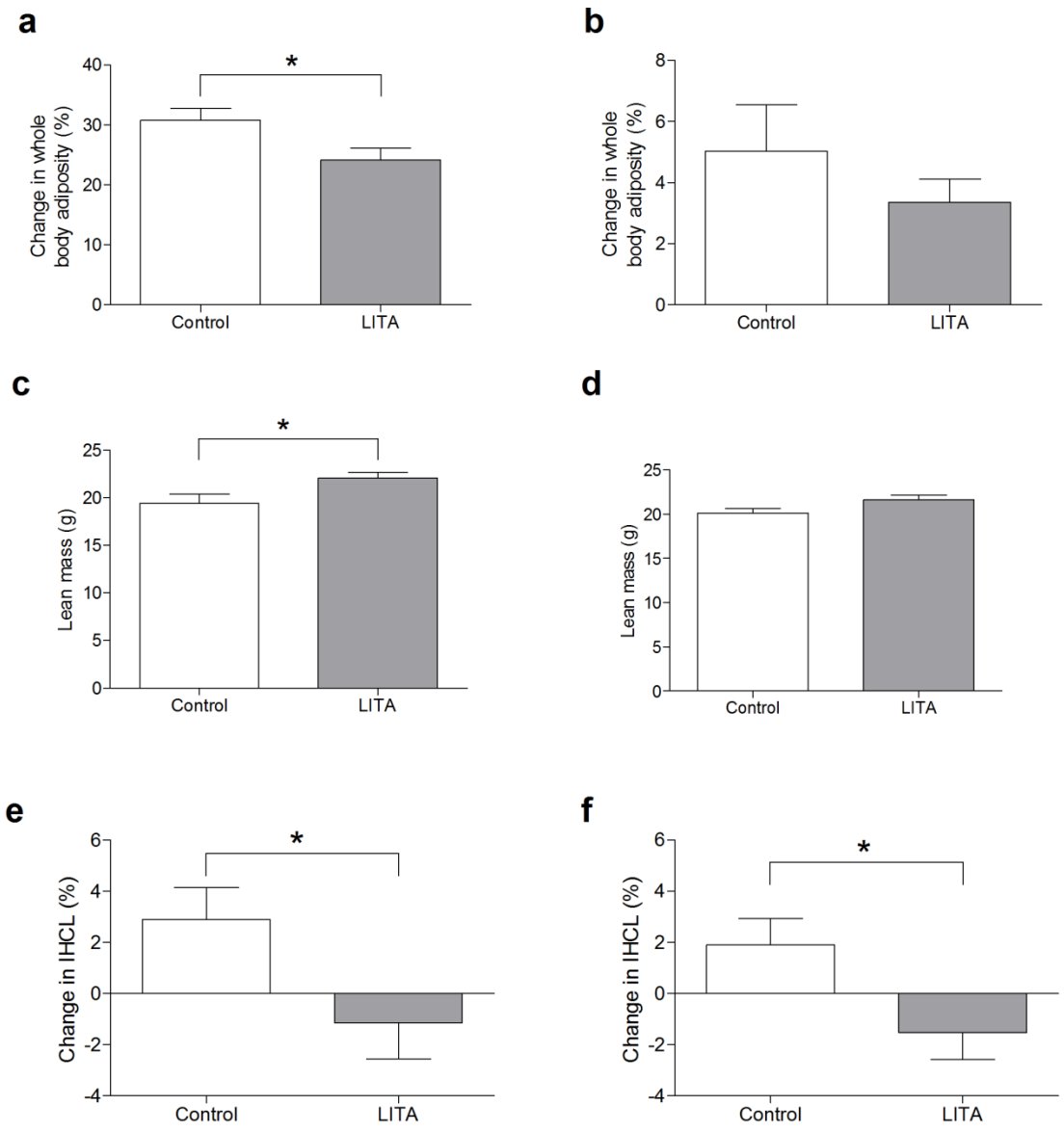
a
Change in whole body adiposity (%)
40
30
20
10
0
*
Control
LITA
b
Change in whole body adiposity (%)
8
6
4
2
0
Control
LITA
c
Lean mass (g)
25
20
15
10
5
0
*
Control
LITA
d
Lean mass (g)
25
20
15
10
5
0
Control
LITA
e
Change in IHCL (%)
6
4
2
0
-2
-4
*
Control
LITA
f
Change in IHCL (%)
6
4
2
0
-2
-4
*
Control
LITA

1

2

Figure 2

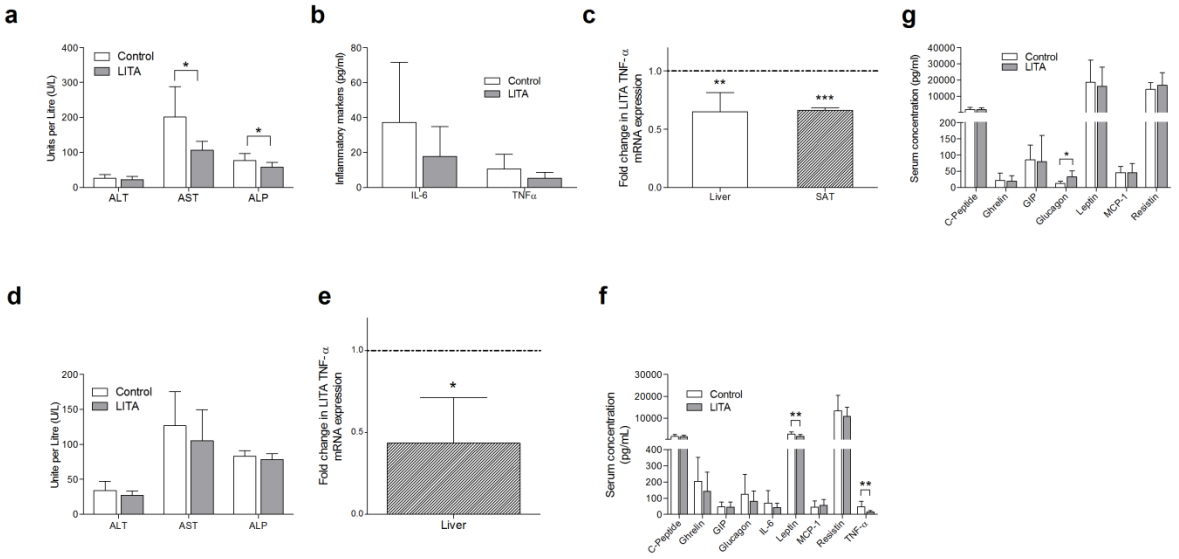
a
Units per Litre (U/L)
Control
LITA
ALT
AST
ALP
b
Inflammatory markers (pg/ml)
IL-6
TNFα
c
Fold change in LITA TNF-α mRNA expression
Liver
SAT
g
Serum concentration (pg/ml)
C-Peptide
Ghrelin
GIP
Glucagon
Leptin
MCP-1
Resistin
d
Units per Litre (U/L)
e
Fold change in LITA TNF-α mRNA expression
Liver
f
Serum concentration (pg/mL)
C-Peptide
Ghrelin
GIP
Glucagon
IL-6
Leptin
MCP-1
Resistin
TNF-α

Figure 3

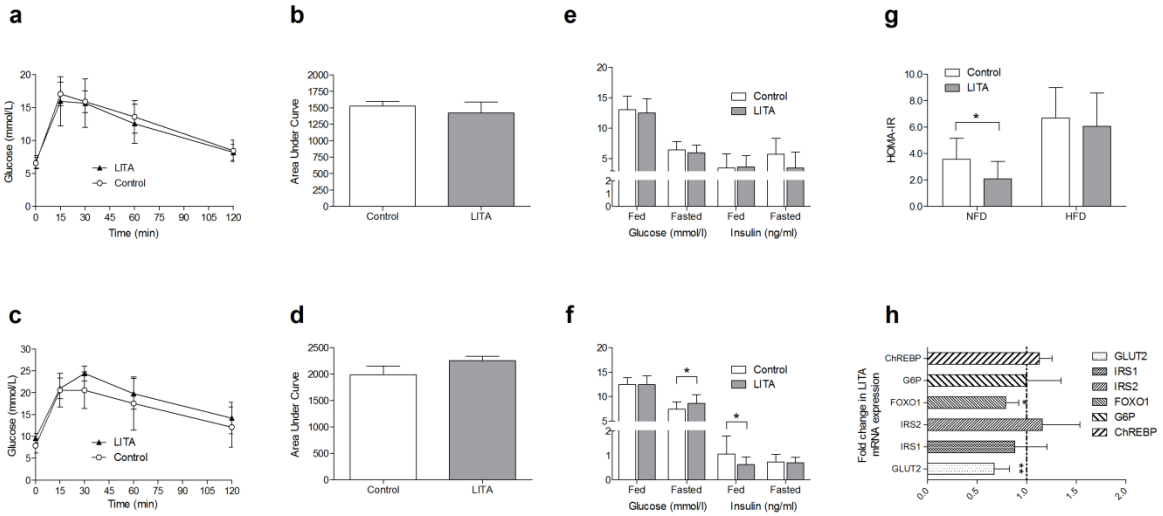
a
b
e
g
Glucose (mmol/L)
Time (min)
LITA
Control
Area Under Curve
Control
LITA
Glucose (mmol/l)
Insulin (ng/ml)
Fed
Fasted
HOMA-IR
NFD
HFD
c
d
f
h
Fold change in LITA mRNA expression
ChREBP
G6P
FOXO1
IRS2
IRS1
GLUT2

Figure 4

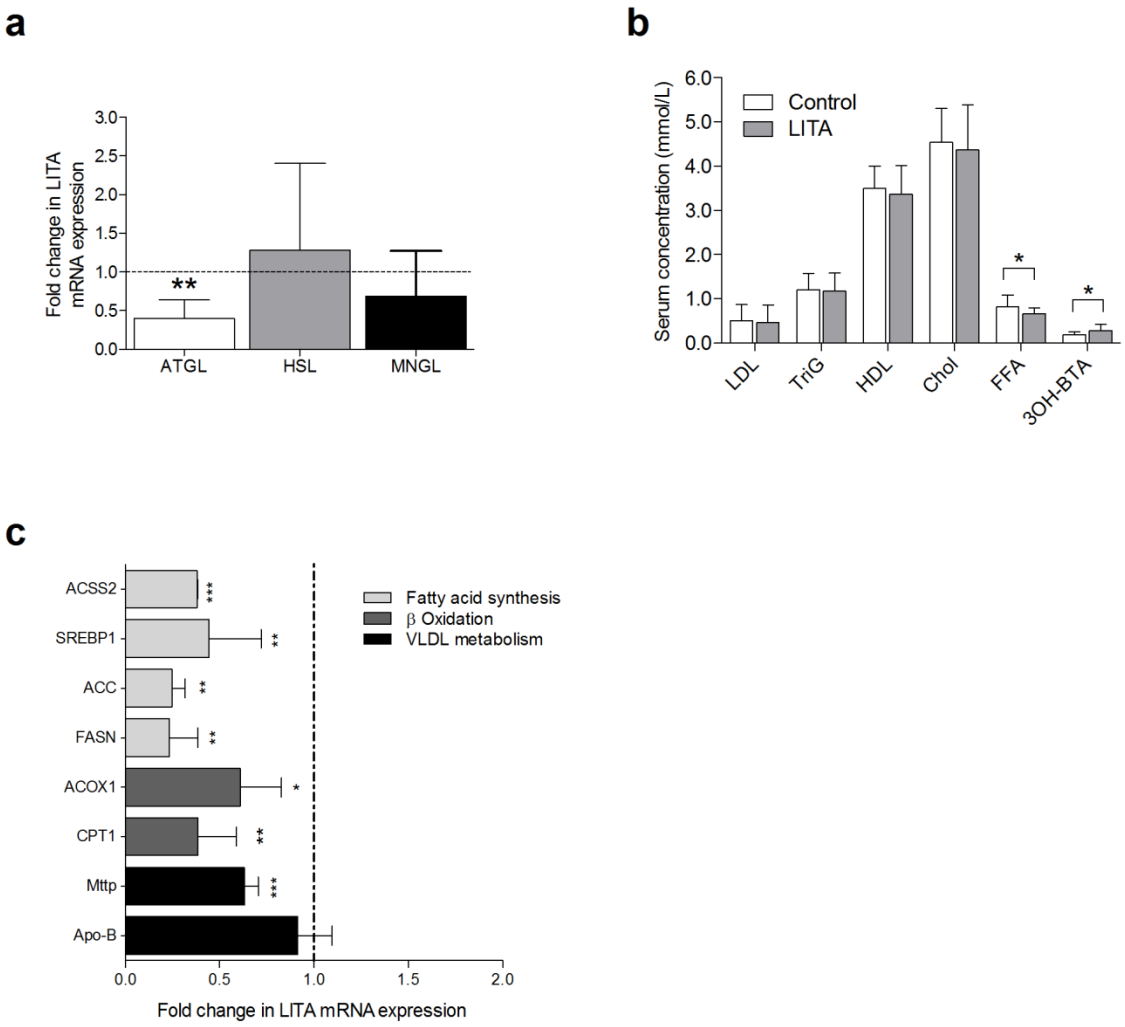
a
Fold change in LITA mRNA expression
3.0
2.5
2.0
1.5
1.0
0.5
0.0
**
ATGL
HSL
MNGL
b
Serum concentration (mmol/L)
6.0
5.0
4.0
3.0
2.0
1.0
0.0
Control
LITA
*
*
LDL
TriG
HDL
Chol
FFA
3OH-BTA
c
ACSS2
SREBP1
ACC
FASN
ACOX1
CPT1
Mttp
Apo-B
***
**
**
**
*
**
***
Fatty acid synthesis
β Oxidation
VLDL metabolism
0.0
0.5
1.0
1.5
2.0
Fold change in LITA mRNA expression

1

2

Figure 5

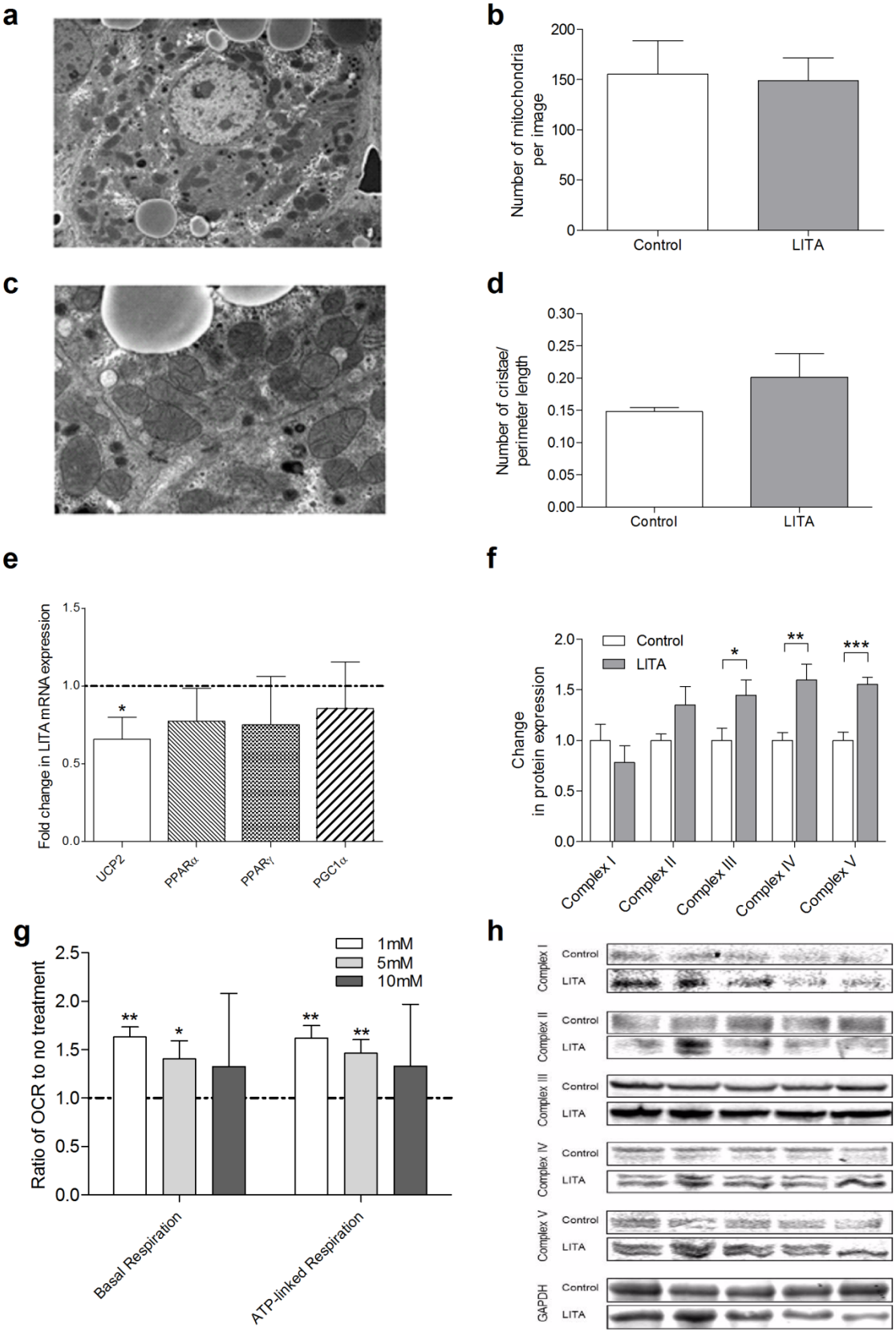
a
b
Number of mitochondria per image
200
150
100
50
0
Control
LITA
c
d
Number of cristae/ perimeter length
0.30
0.25
0.20
0.15
0.10
0.05
0.00
Control
LITA
e
Fold change in LITA mRNA expression
1.5
1.0
0.5
0.0
*
UCP2
PPARα
PPARγ
PGC1α
f
Change in protein expression
2.0
1.5
1.0
0.5
0.0
Control
LITA
*
**
***
Complex I
Complex II
Complex III
Complex IV
Complex V
g
Ratio of OCR to no treatment
2.5
2.0
1.5
1.0
0.5
0.0
1mM
5mM
10mM
**
*
**
**
Basal Respiration
ATP-linked Respiration
h
Complex I
Complex II
Complex III
Complex IV
Complex V
GAPDH
Control
LITA

1
2

Figure 6

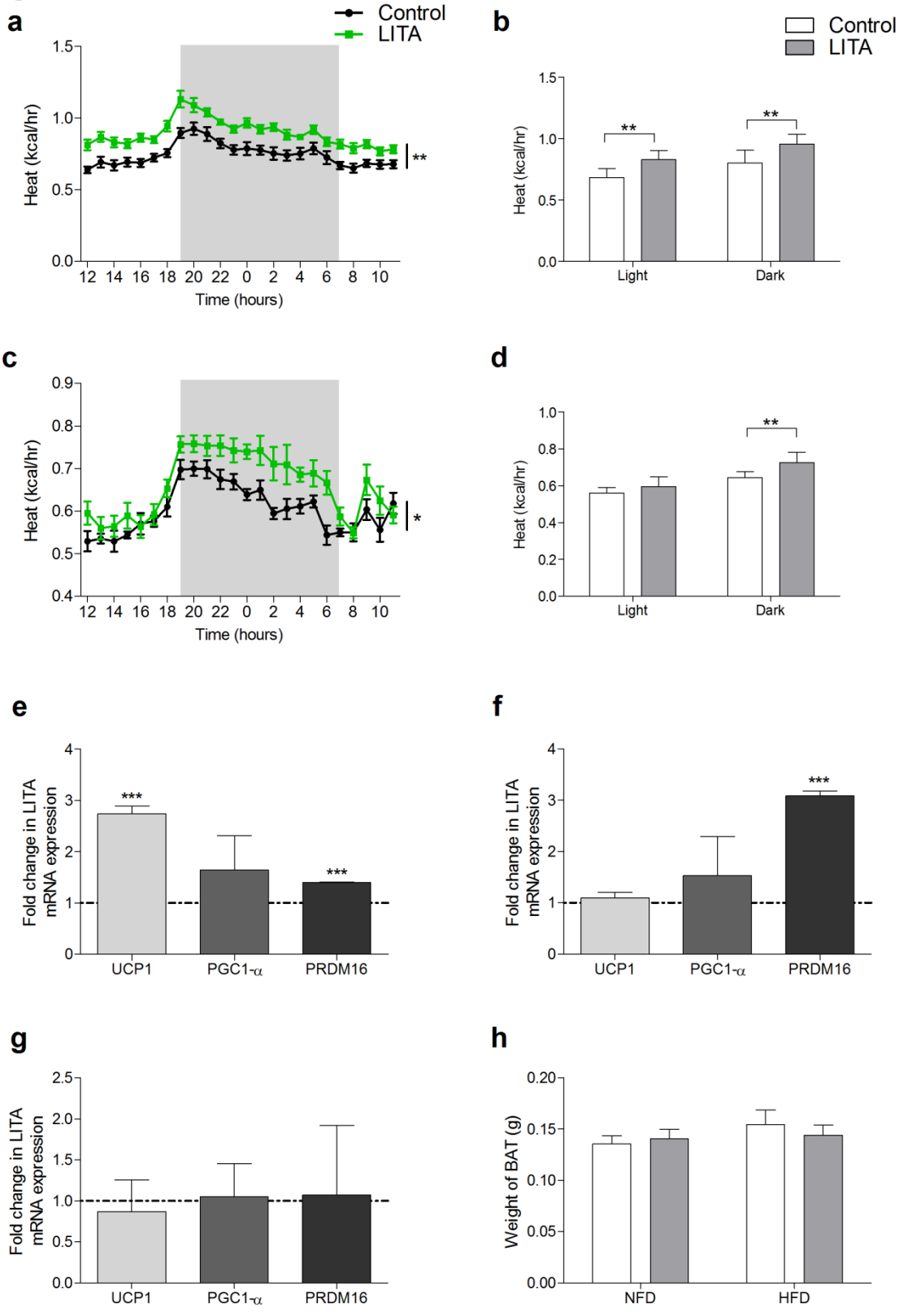
a
Control
LITA
Heat (kcal/hr)
Time (hours)
**
b
Control
LITA
Heat (kcal/hr)
Light
Dark
**
**
c
Heat (kcal/hr)
Time (hours)
*
d
Heat (kcal/hr)
Light
Dark
**
e
Fold change in LITA mRNA expression
***
***
UCP1
PGC1-α
PRDM16
f
Fold change in LITA mRNA expression
***
UCP1
PGC1-α
PRDM16
g
Fold change in LITA mRNA expression
UCP1
PGC1-α
PRDM16
h
Weight of BAT (g)
NFD
HFD

1